Journal of Quantitative Spectroscopy & Radiative Transfer 164 (2015) 89–96

Contents lists available at ScienceDirect

Journal of Quantitative Spectroscopy & Radiative Transfer

journal homepage: www.elsevier.com/locate/jqsrt

Plasma diagnostics from self-absorbed doublet lines in laser-induced breakdown spectroscopy

C.A. D'Angelo*, M. Garcimuño, D.M. Díaz Pace, G. Bertuccelli

Centro de Investigaciones en Física e Ingeniería del Centro de la Provincia de Buenos Aires (CONICET-UNCPBA), Campus Universitario, Fac. de Cs. Exactas (B7000GHG) Tandil, Buenos Aires, Argentina

ARTICLE INFO

Article history:
Received 6 March 2015
Received in revised form
11 May 2015
Accepted 28 May 2015
Available online 6 June 2015

Keywords:
Laser-induced breakdown spectroscopy
LIBS
Self-absorption
Plasma characterization

ABSTRACT

In this paper, a generalized approach is developed and applied for plasma characterization and quantitative purposes in laser-induced breakdown spectroscopy (LIBS) experiences by employing a selected pair of spectral lines belonging to the same multiplet. It is based on the comparison between experimental ratios of line parameters and the theoretical calculus obtained under the framework of a homogeneous plasma in local thermodynamic equilibrium. The applicability of the method was illustrated by using the atomic resonance transitions 279.55–280.27 nm of Mg II, which are usually detected in laser-induced plasma (LIP) during laser ablation of many kinds of targets. The laser induced plasmas were produced using a Nd:YAG laser from a pressed pellet of powdered calcium hydroxide with a concentration of 300 ppm of Mg. The experimental ratios for peak intensities, total intensities and Stark widths were obtained for different time windows and matched to the theoretical calculus. The temperature and the electron density of the plasma, as well as the Mg columnar density (the atom/ion concentration times the length of the plasma along the line-of-sight), were determined. The results were interpreted under the employed approach.

1. Introduction

Laser-induced breakdown spectroscopy (LIBS) is an analytical technique that uses a laser-induced plasma (LIP) as emission spectroscopic source for analytical purposes [1–3]. Nowadays, LIBS technique is a very active field of research due to its inherent advantages with respect to other well-established techniques to perform elemental analysis of a widespread variety of samples such as liquids, solids, gases, and aerosols [4]. Nevertheless, spectrochemical LIBS analysis is not straightforward because the spectroscopic emission of the LIP is determined not only by the concentration of the analyte in the sample, but also by the properties of the plasma itself, which depend on the experimental conditions [5]. In fact, in LIP generated in air at atmospheric pressure, the main issues that have to be taken into account are time evolution, self-absorption, spatial inhomogeneity, and matrix effects. Valuable insight about these physical processes can be achieved by characterizing the plasma through the determination of its physical parameters, such as temperature, electron density, and density of the present species [6]. LIP diagnostics is crucial in order to accomplish the full LIBS potential as analytical method [7].

Traditional methods for plasma characterization in LIBS are based on optically thin plasma emission [8]. However, it is well known that self-absorption of the spectral lines is one of the main systematic errors in plasma diagnostics as well as in quantitative analysis. The problem of evaluating

*Correspondence to: Pinto 399, (B7000GHG) Tandil, Buenos Aires, Argentina.
Tel.: +54 249 4439660, +54 249 4439661; fax: +54 249 4439669.
E-mail address: cdangelo@exa.unicen.edu.ar (C.A. D'Angelo).

http://dx.doi.org/10.1016/j.jqsrt.2015.05.014
0022-4073/

and compensating self-absorption has been widely discussed in the literature (see [9] and refs. therein). From an experimental point of view, self-absorption can be overcome or reduced by a proper choice of the measurement conditions and/or selection of suitable emission lines [10]. The most common approach is to discard those transitions showing self-absorption at the conditions of measurement, mainly the resonance lines, and thus selecting for the analysis the optically thin transitions. In the curve-of-growth (CoG) method, the specific content of the element of interest is selected in such a way that self-absorption is negligible. In this case, the measurement of several samples with different concentrations is required [11]. Another approach is to generate the plasma with relatively high laser energy under a low pressure atmosphere of an inert gas [12,13]. However, depending on the particular experiment and the analyte, achieving optically thin conditions of measurement can be cumbersome.

Line shape analysis brings useful information about LIP conditions [14]. Hence, methods to account for self-absorption have been reported relying on its effects on the line emission profiles [15–19]. Another well-known procedure to quickly evaluate the occurrence of self-absorption is checking the intensity ratio of a pair of lines belonging to the same multiplet [20]. A reduction in the observed intensity ratio, i.e.: the stronger line relative to the weaker line, with respect to the theoretical ratio expected in optically thin conditions indicates that self-absorption is present. As an example, in a previous work, we employed the measured intensities of the Mg II doublet (279.55–280.27 nm) to check if the spectra were emitted in optically thin regime and, then, be used to obtain the electron density of the plasma [21].

In LIP, for a given element and given experimental conditions, self-absorption varies with time due to the variation of the thermodynamic parameters of the plasma. Consequently, assessing the occurrence of self-absorption for the spectral lines measured is of paramount interest in LIBS experiments aimed at both basic and applied studies. On these steps, the main goal of the present work was employing a selected pair of spectral lines belonging to the same multiplet and affected by self-absorption for the purpose of both quantitative analysis and plasma diagnostics. Although several papers have been published on this subject, LIP diagnostics in optically thick conditions is still interesting to get valuable understanding about these complex sources of radiation. For example, the Mg II resonance spectral lines are useful for astrophysical plasma diagnostics and modeling [22].

An approach was developed to accomplish a complete plasma characterization, i.e. temperature, electron density and *Nl* parameter (the particle density times the optical length of the plasma along the line-of-sight). It is based on comparing the experimental ratios of peak intensities, total intensities, and widths with the corresponding theoretical values calculated in a framework of a homogeneous plasma in local thermodynamic equilibrium (LTE). The method was applied to the atomic resonance transitions 279.55–280.27 nm of Mg II, which are usually detected in LIBS experiences carried out with many kinds of targets and suffer generally of a moderate to strong self-absorption. It will be useful to those applications where a rapid plasma characterization is required and/or calibration curves are not practicable for quantitative analysis because either standards are not available (i.e. unique, unknown, complex or expensive samples) or the measurements are affected by strong matrix effects. Furthermore, some insight about the physical processes involved, such as self-absorption and spatial inhomogeneity, was obtained.

2. Theoretical: spectral line emission from a homogeneous plasma in LTE

We consider a cylinder-symmetrical homogeneous plasma in local thermodynamic equilibrium (LTE). The spectrally resolved intensity I_λ (J s^{-1} m^{-2} sr^{-1} nm^{-1}) of an emission line, integrated along the line of sight, is given by solution to the equation of radiation transfer [22]

$$I_\lambda = U_\lambda(T)(1-e^{-\tau_\lambda}) \tag{1}$$

where U_λ (J s^{-1} m^{-2} sr^{-1} nm^{-1}) is the distribution for blackbody radiation, and τ_λ (adimensional) is the optical depth, which determines the degree of self-absorption of the line. The optical depth can be expressed by [8]

$$\tau_\lambda = \kappa(\lambda)l = \kappa_t(T)N\, l\, P(\lambda) \tag{2}$$

where $\kappa_t(T)$ (m^2 s^{-1}) is a coefficient that depends on the atomic parameters of the transition and that can be calculated if the plasma temperature is known. Namely,

$$\kappa_t(T) = \frac{\lambda_0^2 g_j A_{ji}}{4Q(T)} e^{-\frac{E_i}{kT}}\left[1-e^{-\frac{(E_j-E_i)}{kT}}\right] \tag{3}$$

where the indexes j and i refer to upper and lower quantum levels of the transition, T (K) is the plasma temperature, λ_0 (m) is the central wavelength of the line, g_j (adimensional) is the degeneracy of the upper energy level, Aji (s^{-1}) is the transition probability, $Q(T)$ (dimensionless) is the atomic partition function, E_i,E_j (eV) are the quantum energy levels, k (J K^{-1}) is the Boltzmann constant, N (m^{-3}) is the density of the emitting element in the plasma, l (m) is the absorption path length, and $P(\lambda)$ (s) is the intrinsic line profile.

The different broadening mechanisms existing in the LIP need to be evaluated to calculate the line profile in Eq. (2). Due to the high electron density present in LIP, the Stark effect is the dominating line-broadening mechanism [23]. Therefore, the line profile is expressed by the Lorentzian function

$$P(\lambda) = \frac{\lambda_0^2}{4\pi^2 c}\frac{w}{\left[(\lambda-\lambda_0)^2+(w/2)^2\right]} \tag{4}$$

where w(m) is the line FWHM given by the Stark width of the line, and c (m s^{-1}) is the speed of light.

In LTE, the ratio of the number densities of species with consecutive ionization stages is given by the Saha equation [24],

$$S_{z-1,z} \equiv \frac{N_e N^z}{N^{z-1}} = 6.04\times 10^{21}\frac{Q^z}{Q^{z-1}} kT^{3/2} e^{-\frac{E_\infty^{z-1}}{kT}}\ \mathrm{m}^{-3} \tag{5}$$

where N_e (m^{-3}) is the electron density of the whole plasma and E_∞^{z-1} (eV) is the ionization energy of the species $z-1$. The

superscript z refers to the ionization degree of the species ($z=0$ for neutral atoms, $z=1$ for singly ionized atoms, etc.).

3. Experimental

3.1. Experimental setup

The experimental setup is based on a monochromator with good spectral resolution allowing a detailed measurement of individual line profiles. It has been used previously, so only a brief description is given here [17–19]. The LIP was generated in air at atmospheric pressure by focusing a Nd:YAG laser (Continuum Surelite II, $\lambda=1064$ nm, 7 ns pulse FWHM, 100 mJ/pulse, repetition rate 2 Hz) at right angles onto the sample surface using a lens of 10 cm focal length. The light emitted by the plasma from its brightest central region was collected at right angles to the laser beam direction by using a quartz lens of 20 cm focal length imaged on the entrance slit (50 μm-width) of a monochromator (Jobin Yvon THR 1500, Czerny–Turner configuration, resolution 0.001 nm in double pass at $\lambda=300$ nm, focal length 1.5 m, grating of 2400 lines/mm). The detector was a photomultiplier (PM) whose signal was time resolved and box-car averaged. The line profiles were scanned moving the diffraction grating of the monochromator controlled by software and synchronized with data acquisition and laser firing. Each experimental point of the emission profile was averaged for 3 laser shots to improve the signal-to-noise ratio. The instrumental function was described by a Gaussian function with an estimated FWHM of 0.005 nm for the 50 μm-width entrance/exit slits and $\lambda=280$ nm. The sample used was fixed to a rotary holder and consisted of a pressed pellet of finely powdered calcium hydroxide prepared in the laboratory with a Mg concentration of 300 ppm. The emission intensities of Mg II doublet lines 279.55 nm and 280.27 nm were measured at 9 time windows during the plasma lifetime ranging from 2 μs to 10 μs with a fixed gate width of 30 ns. The atomic data of the lines are listed in Table 1. The delay time with respect to the laser pulse was varied in the range 2–10 μs.

3.2. The model

In order to simulate the emission line profiles, we employed the basic equations of Section 2, as well as standard statistical distributions. Moreover, the following assumptions were made on specific properties of the plasma:

(i) In real LIP generated in atmospheric conditions, spatial gradients of the plasma parameters exist inside the plume. This fact can be accounted by using a more elaborated framework of an inhomogeneous plasma. Nevertheless, this will involve many parameters thus reducing their practical applicability. Therefore, a simple model of a homogeneous plasma in LTE was considered to describe the line profiles. Moreover, when spatially-integrated line intensities are measured, the plasma parameters have apparent values representing a population average of the real spatial distributions within the plasma region from which the spectral lines are emitted [25].

(ii) In a previous work, we studied the time dependence of the temperature and the electron density for LIP generated in similar conditions as here and from the same kind of samples [17]. Both the parameters were determined using Mg I–II lines and the results were presented in graphical form. In order to ease the use of those results, we derived an empirical relation linking the plasma electron density N_e (m^{-3}) with the temperature kT (eV) as follows:

$$N_e(kT) = y_0 + a\exp\left(\frac{kT - x_0}{b}\right) \tag{6}$$

with

$y_0 = 2.63\times10^{23}\ m^{-3}$
$x_0 = 1.33$ eV
$a = 8.74\times10^{23}\ m^{-3}$
$b = 0.33$ eV

As shown in Fig. 1, this expression reproduces the experimental data in the temperature range 1.8–0.5 eV with a high correlation ($R^2=0.998$). The estimated error for the electron density was 5–10%.

(iii) The total Mg number density N_{Mg} (m^{-3}) was supposed to be constant along the line of sight of the plasma. Furthermore, we considered that, for the typical values of temperatures and electron densities of LIP in our experiment (i.e.: $kT\sim1$ eV and $N_e\sim10^{23}\ m^{-3}$), the total density of Mg species in the plasma is N_{Mg} (m^{-3})$=N_{MgI}+N_{MgII}+N_{MgIII}$. Hence, since LTE holds, the number densities of the different ionization species (m^{-3}) can be calculated using the Saha equation (4). Namely,

$$N_{Mg\ I} = \frac{N_{Mg}\,N_e}{N_e+S_{12}}\left[1-\frac{S_{12}\,S_{23}}{N_e(N_e+S_{12})-S_{12}\,S_{23}}\right] \tag{7}$$

$$N_{Mg\ II} = \frac{N_{Mg}\,S_{12}}{N_e+S_{12}}\left[1-\frac{S_{12}\,S_{23}}{N_e(N_e+S_{12})-S_{12}\,S_{23}}\right] \tag{8}$$

$$N_{Mg\ III} = \frac{N_{Mg}S_{12}S_{23}}{N_e(N_e+S_{12})-S_{12}S_{23}} \tag{9}$$

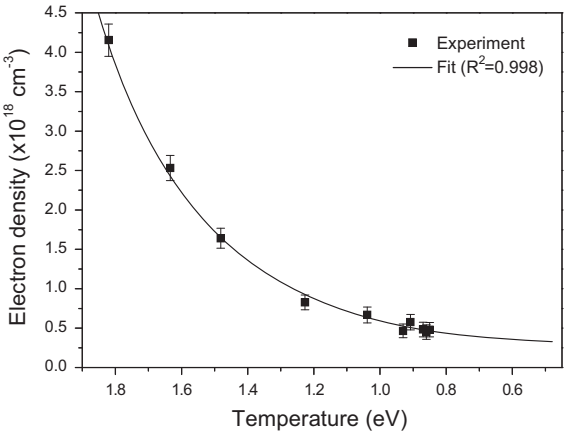

Fig. 1. Electron density of the laser-induced plasma at different temperatures.

where $S_{z-1,z}$ is the Saha equation (5) for the species z and $z-1$. As an example, written in practical units,

$$S_{12} = N_e \frac{N_{Mg\ II}}{N_{Mg\ I}} = \frac{Q_{Mg\ II}}{Q_{Mg\ I}} 6.042 \times 10^{21} (kT)^{3/2} e_{-E_{\infty}^{Mg\ I}/kT}\ \mathrm{m}^{-3} \quad (10)$$

with $E_{\infty}^{Mg\ I} = 7.646$ eV.

Fig. 2 shows the relative number densities of the different ionization stages with respect to the total Mg density for a typical decreasing range of temperatures reached in LIBS experiments, calculated by employing Eqs. (6) and (7)–(9). It is observed that ionization stages higher than two do not contribute to the total Mg density. Moreover, for temperatures >0.8 eV the density of Mg II is larger than the density of Mg I, while the density of Mg III is small ($<6\%$). On the other hand, for temperatures <0.8 eV the density of Mg II is lower than the density of Mg I.

(iv) In typical LIBS experiences, Stark broadening is the predominant mechanism that determines the Lorentzian contribution to line profiles [23]. It is proportional to the electron number density, namely,

$$w_{Stark} = 2w \frac{N_e}{N_e^{Ref}}\ \mathrm{nm} \quad (11)$$

where w (nm) is the electron impact half width and N_e^{Ref} (m^{-3}) is a reference electron density, usually 10^{22} or $10^{23}\ \mathrm{m}^{-3}$[26].

Our calculations employ the following home-made computer algorithm. The input parameters are the experimental line and its spectroscopic data. After that, a range of values for the plasma temperature (kT) and the total columnar density ($N_{Mg}l$) are set by the user. Then, the line intensity profiles for the Mg transitions are calculated using Eqs. (1)–(11). The intrinsic line profiles are convoluted with the instrumental function of the monochromator. Finally, the results obtained for the simulated lines are their total intensity, peak intensity, and width, from which the corresponding theoretical ratios are computed as a function of kT and the product $N_{Mg}l$. An advantage of the present approach is that it does not require the use of a set of reference samples with several concentrations of the element of interest and it does not require the knowledge of the detector spectral efficiency.

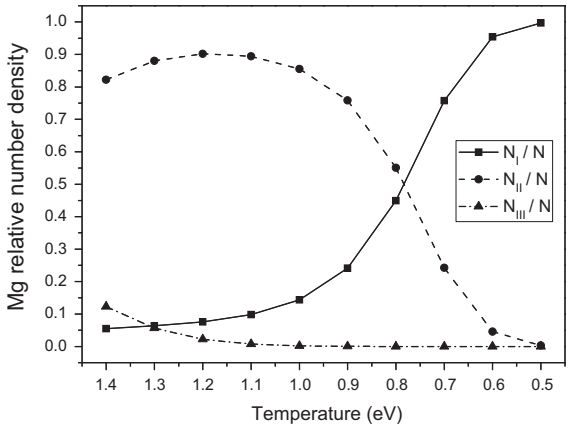

Fig. 2. Number densities of neutral (N_I), singly-ionized (N_{II}) and doubly-ionized (N_{III}) atoms for Mg, normalized to the total Mg density (N), as a function of temperature.

4. Results and discussion

The developed approach was applied to compute the peak intensity ratios, total intensity ratios, and width ratios for the Mg II line 279.55 nm with respect to the Mg II line 280.27 nm by running the algorithm for $kT = 0.5$–1.4 eV and $N_{Mg}l = 10^{15}$–$10^{20}\ \mathrm{m}^{-2}$. This models a LIBS experiment in which these lines are recorded at several time windows characterized by different plasma temperatures from samples with a varying Mg concentration. The output of the algorithm is shown in Fig. 3, where the calculated ratios are shown as a function of $N_{Mg}l$ for the different plasma temperatures.

In Fig. 3a and b, similar trends are observed for both the peak and total intensity ratios. For a given plasma temperature, the ratios decrease as $N_{Mg}l$ increases from a value of 2, corresponding to optically thin plasma condition, up to a value of 1, for optically thick condition. Moreover, it can be observed that the change from optically thin to optically thick regime is more abrupt for the peak ratios (Fig. 3a) with respect to the total intensity ratios (Fig. 3b). This can be attributed to the fact that self-absorption starts in the peak of the line and, as the optical depth increases with the elemental concentration, it spreads out progressively towards the wings, which is reflected in the emission intensity. Furthermore, in both the figures the transition to self-absorbed regime occurs at higher values of the parameter Nl for the lower plasma temperature. This feature is more evident in both figures for $kT = 0.5$–0.6 eV, where transition occurs for Nl values one or two orders of magnitude higher than that for the other temperatures. This may be explained because at such temperatures the relative population of Mg II is very low (Fig. 2); thus, a higher Mg concentration is required in order for the self-absorption effects to become noticeable.

In turn, a more complicated trend is observed for the width ratios for the different plasma temperatures (Fig. 3c). For lower Nl values, the width ratios are 1; then, the ratios grow with the Mg density to reach a maximum and, finally, decrease again to 1 for higher Mg densities. In addition, it is observed that the lower the plasma temperature, the rise and decrease take place at higher Nl values. As discussed in the following, this behavior may be mainly explained by the different degrees of self-absorption affecting each line of the Mg II doublet.

With the support of the calculations exposed in Fig. 3, the method developed is based on the spectral differences produced by self-absorption of two lines belonging to the same multiplet since it modifies in a different way the line intensity, peak intensity and line width because of their dependence on the plasma parameters (i.e.: kT, N_e, Nl). However, in the two limits of optically thin or complete optically thick conditions this spectroscopic magnitudes are not dependent on the plasma parameters. Next, the outputs of the model are compared with measurements from a real LIBS experiment.

To verify experimentally the applicability of the model described in Section 3.2, it was applied to characterize LIP

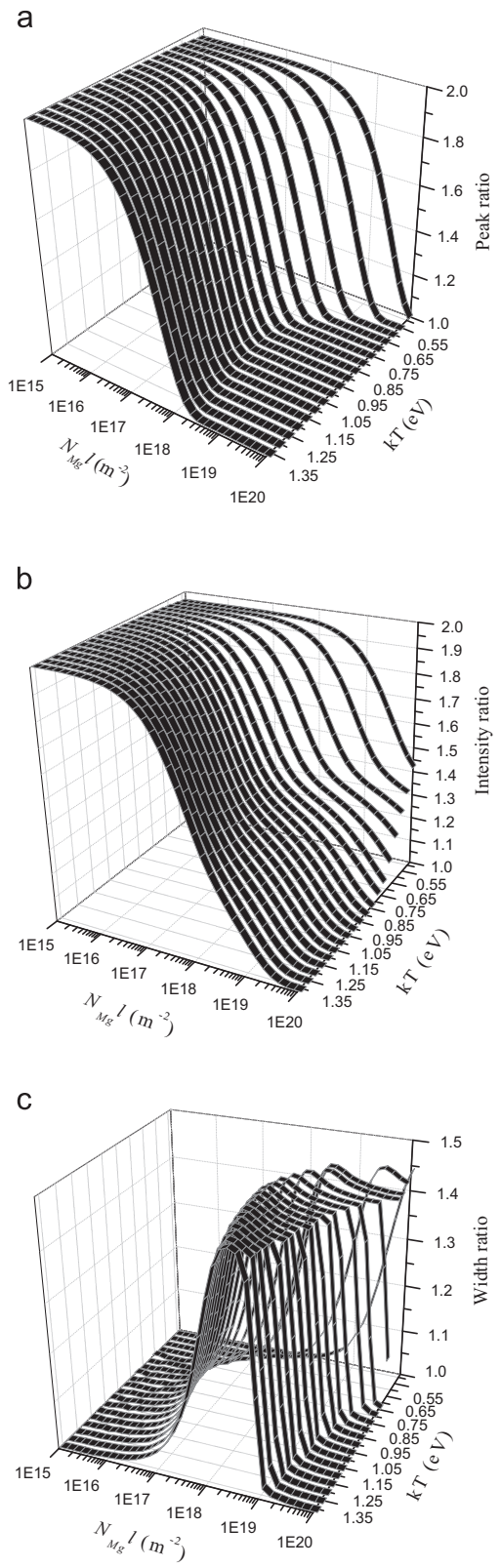

Fig. 3. Theoretical peak ratios (a), intensity ratios (b) and width ratios (c) for Mg II line 279.55 nm with respect to Mg II line 280.27 nm computed under the framework used in the present work as a function of Mg columnar density and temperature.

by employing the Mg II doublet 279.55–280.27 nm. To this aim, both the resonance spectral lines were recorded with different time windows in the range 2–10 μs. The peak intensities, total intensities (wavelength integrated), and widths of the Mg II lines were determined from their measured profiles, as described in Section 3.2. Then, the respective experimental ratios were compared with the theoretical calculus of the model proposed.

In the ideal case, a single value of the $N_{Mg}l$ product and a finite range of plasma temperature are expected to describe all the experimental points. In practice, some differences between the parameters kT and $N_{Mg}l$ determined for each of the ratios occurred because of the experimental errors in the measurement of the line parameters. Hence, an automatic routine to find the best fitting for all the curves simultaneously is a cumbersome task due to a tradeoff taking place between the different values of the parameters to be optimized. Therefore, the values for which a good agreement between theory and experiment occurred were found by visual comparison. In this way, the final set of values of the plasma parameters obtained for the time windows analyzed in this work are listed in Table 2. These results were deduced from spectra obtained via integration of the measured emission intensity along the line of sight from a near homogeneous plasma. Thus, the parameters have apparent values corresponding to population averages [27]. The electron density was in all cases above the critical value for the existence of LTE according to Mc Whirter criterion [6].

The experimental and theoretical results are compared in Fig. 4. The experimental ratios are assigned to the different time windows in the upper x-axis, while the plasma temperatures obtained are indicated in the lower x-axis. The errors for the experimental ratios were estimated from the propagation of the individual errors of the different line parameters. It is observed that, in our experimental conditions, the results are in good agreement with the theoretical curves with the exception of two points in Fig. 4a and c, corresponding to the lower temperatures. An explanation for this discrepancy is given below.

The extent of self-absorption affecting each line is determined by its optical depth which, as discussed in a previous paper [18], is determined by the following main factors: the plasma temperature, the spectroscopic features of the line, the columnar density, and the line shape. Initially, the columnar density $N_{Mg}l$ is related to the ablation process which depends on the laser irradiance and the properties of the sample surface [29]. Then, as stated in [30], as a consequence of the growth of the plasma volume due to the rapid plasma expansion the $N_{Mg}l$ value increases due to an increment of the optical path dimension and decreases due to a diminution of the species density. The net result is a net reduction of the columnar density and, thereby, of the optical depth. As shown in [18], this effect is more pronounced during the expansion stage of the plume at early times of its evolution. On the other hand, at longer times where the plasma expansion slowed down the Nl product remains approximately constant. In our experimental conditions, a single value of $N_{Mg}l = (3 \pm 1) \times 10^{20}\,\mathrm{m}^{-2}$ describes well the

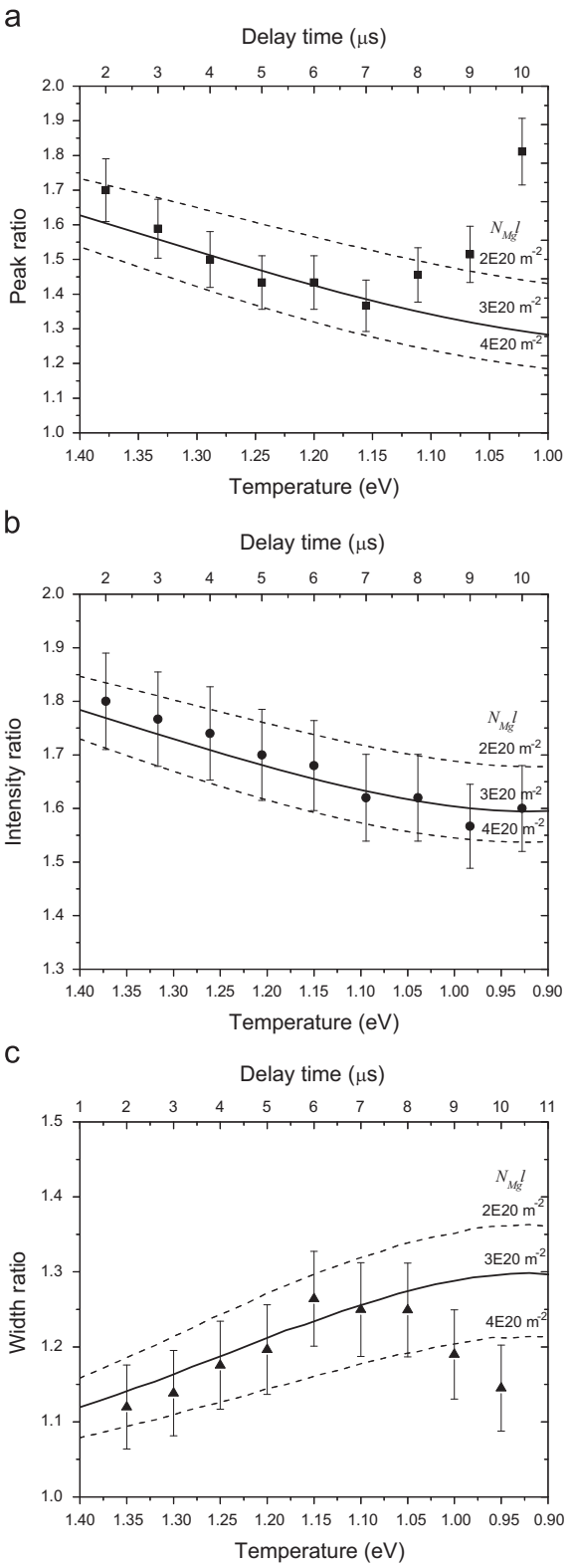

Fig. 4. Experimental peak ratios (a), intensity ratios (b) and width ratios (c) for Mg II line with respect to Mg II line 280.27 nm recorded at different time windows. The solid and dashed lines represent the theoretical curves computed for different Mg columnar densities under the framework used in the present work.

experimental ratios within the error, except for the mentioned pair of points for the lower temperatures in Fig. 4a and c. Thus, in our experiment the plasma plume finished its expansion at the delay times recorded.

From the results of Tables 1 and 2, some useful understanding about the physical processes occurring in the LIP, such as self-absorption and spatial inhomogeneity, can be derived by correlating them to the trends of the thermodynamic parameters. The temperature and electron density of the LIP decrease with time as a result of the plasma cooling and recombination, respectively. The range of values for the κ_t coefficients, Stark widths, and maximum optical depths calculated for the Mg II lines are shown in Table 1. The high values of the optical depths evidence the important self-absorption suffered by both the lines at all the time windows measured. Moreover, in the time interval studied, the Mg II density experiments only a slight variation ($<10\%$, Fig. 2) and the κ_t of both lines are approximately constant, while the Stark widths decrease with N_e, as shown in Table 1. This originates a growth of their optical depths and, hence, a higher self-absorption as time progresses, which is evidenced in the decreasing trends of both the peak and the intensity ratios in Fig. 4a and b.

The Stark width of lines belonging to the same multiplet is usually the same within a few percent [20]. Thus, both the lines of the Mg II doublet have approximately the same line profile in Eq.(2). Consequently, their relative self-absorption will be determined only by their κ_t factors, which depend on the line spectroscopic features and the plasma temperature. In our case, $\kappa_t(279.55)/\kappa_t(280.27) \approx 2$ independently of the temperature; therefore, the line 279.55 nm is approximately two times more sensitive to self-absorption than the line 280.27 nm. Since self-absorption causes an additional broadening of the line profiles with respect to the optically thin case, it follows that the line 279.55 nm will experiment a faster broadening than the line 280.27 nm as the Mg II density grows. For the decreasing range of temperature obtained in this work (see Table 2), the k_t factors are constant for both the lines. Thus, their optical depths grow (see Table 1) and originate the increasing trend of their width ratio, as observed in Fig. 4c.

As previously mentioned, the model of a homogeneous plasma fits well with the measurements within the experimental errors, except at the later time windows analyzed in Fig. 4a and c where the experimental ratios show a systematic deviation from the theoretical calculus. In fact, for times of 8–10 μs our model predicted ratios that are either lower (Fig. 4a) or higher (Fig. 4c) than the experimental values obtained. This observation can be explained by the fact that the adopted model does not describe the results very well for intense lines with strong self-absorption, as already described by Aguilera et al. [31] and also observed in a previous work of our group for the Mg resonance lines [17]. In the present study, the results indicate that, for the later times, the optical depths of the lines of the Mg II doublet increased due to the decrease of about one order of magnitude of the electron density of the plasma and thus the effects of plasma inhomogeneity started to be noticeable. A more elaborated approach

Table 1
Spectral lines used to characterize the plasma, with their atomic data (taken from [28]) and κ_t, w_{Stark}, and $\tau_0=\tau(\lambda_0)$ values obtained.

Element	Line (nm)	A_{ji} (10^8 s^{-1})	E_j (eV)	E_i (eV)	g_j	g_i	κ_t (10^{-6} m^2 s^{-1})[a]	w_{Stark} (nm)[a]	τ_0 ($adim$)[a]
Mg II	279.55	2.60	4.434	0	4	2	8.73–8.71	0.707–0.377	820–1331
Mg II	280.27	2.57	4.422	0	2	2	4.33–4.32	0.707–0.377	409–665

[a] Calculated for $kT=1.4$–1.0 eV and $N_e=(1.3$–$0.7\pm0.1)\times10^{24}$ m^{-3}.

Table 2
Range value of the plasma parameters obtained for the delay times analyzed.

t_{Delay} (μs)	kT (eV)	N_e (m^{-3})	$N_{Mg}l$ (m^{-2})
2–10	1.40–1.09 ± 0.05	$(1.3$–$0.7\pm0.1)\times10^{24}$	$(3\pm1)\times10^{20}$

should be used where the plasma parameters take apparent values resulting from the integration over different plasma regions. Thereby, a significant part of the line emission coming from the outer regions with lower optical depths (optically thin conditions) explains why the experimental peak ratios are higher than the values predicted by the homogeneous framework in Fig. 4a. Similarly, the Stark widths of the lines contain important contributions of optically thin regions where the broadening of both Mg II lines is the same causing the observed decrease of the width ratio. In turn, this systematic deviation was not observed for the intensity ratios in Fig. 4b. This may be due to the fact that the line center is more susceptive to spatial gradients of temperature than that of the wings. Therefore, the inhomogeneity effects do not affect appreciably the total intensity ratios measured.

5. Conclusions

In the present paper, an approach was developed for plasma characterization and quantitative purposes based on a model of a homogeneous plasma in LTE. The method is applicable to any pair of lines of the same multiplet with known values of their atomic parameters and affected by self-absorption. Measurements at different time windows are required to assure the variation of self-absorption due to the consequent time evolution of the plasma parameters. Furthermore, it does not need the construction of CoG nor the knowledge of the detector spectral efficiency.

The method was applied to the atomic resonance transitions 279.55–280.27 nm of Mg II but it can be easily extended to other atomic/ionic elements. The matching of theoretical calculus to the experimental ratios provided the set of parameters describing the plasma, i.e.: kT, N_e, and $N_{Mg}l$. These are apparent values corresponding to a population average over the real spatial distributions within the plasma plume.

The line measurements were made at times of plasma evolution in which the plume has almost finished its expansion. At this stage, lower gradients of the parameters existed and a near homogeneous plasma was considered, that is the effects of spatial inhomogeneities on the line profiles can be neglected. The model of a homogeneous plasma described well the measurements for spectral lines showing low to moderate self-absorption. In turn, when self-absorption of the lines is strong, as observed for the later time windows analyzed, the systematic deviation observed for the experimental peak intensities as well as for widths ratios with respect to the theoretical calculus indicated that the effects of plasma inhomogeneity started to be noticeable again. At this stage of plasma lifetime, the model of a homogeneous plasma does not describe properly intense lines affected by strong self-absorption; i.e.: with high optical depths. On the other hand, this does not occur for the experimental total intensity ratios due to their low sensitivity to spatial gradients of temperature, which make it more reliable to evaluate self-absorption. Overall, in our experimental conditions, the good general agreement found between theory and experiment supported the suitability of the model for plasma diagnostics employing doublet lines affected by low to moderate self-absorption.

Acknowledgments

This work was supported by Comisión de Investigaciones Científicas de la Provincia de Buenos Aires (CICPBA) and Consejo Nacional de Investigaciones Científicas y Técnicas (CONICET).

References

[1] Miziolek AW, Palleschi V, Schechter I. Laser induced breakdown spectroscopy. Cambridge: Cambridge University Press; 2006.
[2] Cremers DA, Radziemski LJ. Handbook of laser-induced breakdown spectroscopy. Chichester: Wiley; 2006.
[3] Singh JP, Thakur SN. Laser-induced breakdown spectroscopy. Amsterdam: Elsevier; 2007.
[4] Winefordner JD, Gornushkin IB, Correll T, Gibb E, Smith BW, Omenetto N. Comparing several atomic spectrometric methods to the super stars: special emphasis on laser induced breakdown spectrometry, LIBS, a future super star. J Anal At Spectrosc 2004;19:1061–83.
[5] Tognoni E, Palleschi V, Corsi M, Cristoforetti G, Omenetto N, Gorhushkin I, et al. From sample to signal in laser-induced breakdown spectroscopy: a complex route to quantitative analysis. In: Miziolek AW, Palleschi V, Schechter I, editors. Laser-induced breakdown spectroscopy (LIBS) fundamentals and applications. New York, USA: Cambridge University Press; 2006. p. 122–70.
[6] Aragón C, Aguilera JA. Characterization of laser induced plasmas by optical emission spectroscopy: a review of experiments and methods. Spectrochim Acta Part B 2008;63:893–916.
[7] Hahn DW, Omenetto M. Laser-induced breakdown spectroscopy (LIBS), Part I: Review of basic diagnostics and plasma–particle interactions: still-challenging issues within the analytical plasma community. Appl Spectrsc 2010;65:335A–66A.
[8] Aragón C, Bengoechea J, Aguilera JA. Influence of the optical depth on spectral line emission from laser-induced plasmas. Spectrochim Acta Part B 2001;56:619–28.
[9] Cristoforetti G, Tognoni E. Calculation of elemental columnar density from self-absorbed lines in laser-induced breakdown spectroscopy:

a resource for quantitative analysis. Spectrochim Acta Part B 2013;79–80:63–71.
[10] Bengoechea J, Aguilera JA, Aragón C. Application of laser-induced plasma spectroscopy to the measurement of Stark broadening parameters,. Spectrochim Acta Part B 2006;61:69–80.
[11] Aragón C, Peñalba F, Aguilera JA. Curves of growth of neutral atom and ion lines emitted by a laser induced plasma. Spectrochim Acta Part B 2005;60:879–87.
[12] Gomba JM, D'Angelo C, Bertuccelli D, Bertuccelli G. Spectroscopic characterization of laser induced breakdown in Al–Li alloys samples for quantitative determination of traces. Spectrochim Acta Part B 2001;56:695–705.
[13] Kuzuya M, Aranami H. Analysis of a high-concentration copper in metal alloys by emission spectroscopy of a laser-produced plasma in air at atmospheric pressure. Spectrochim Acta Part B 2000;55:1423–30.
[14] Thorne A, Litzén U, Johansson S. The width and shape of spectral lines. In: Spectrophysics: principles and applications. Berlín: Springer; 1999, p. 187–208.
[15] Amamou H, Bois A, Ferhat B, Redon R, Rosetto B, Matheron P. Correction of self-absorption spectral line and ratios of transition probabilities for homogeneous and LTE plasma. J Quant Spectr Radiat Transfer 2002;75:747–63.
[16] Di Rocco HO, Brédice F, Palleschi V. The calculation of the optical depths of homogeneous plasmas: analytical, experimental, and numerical considerations. Appl Spectrosc 2011;65:1–5.
[17] Díaz Pace DM, D'Angelo CA, Bertuccelli G. Calculation of optical thicknesses of magnesium emission spectral lines for diagnostics of laser-induced plasmas. Appl Spectrosc 2011;65:1202–12.
[18] Díaz Pace DM, D'Angelo CA, Bertuccelli G. Study of self-absorption of emission magnesium lines in laser-induced plasmas on calcium hydroxide matrix. IEEE Trans Plasma Sci 2012;40:898–908.
[19] Pace DM Díaz. Laser-induced plasma characterization using line profile analysis of chromium neutral atom and ion transitions. J Quant Spectrosc Radiat Transfer 2013;129:254–62.
[20] Konjevic N, Ivkovic M, Jovicevic S. Spectroscopic diagnostics of laser-induced plasmas. Spectrochim Acta Part B 2010;65:593–602.
[21] Garcimuño M, Díaz Pace DM, Bertuccelli G. Laser-induced breakdown spectroscopy for quantitative analysis of copper in algae. Opt Laser Technol 2013;47:26–30.
[22] Bukvić S, Srećković A, Djeniže S. Mg II h and k lines Stark parameters. New Astron 2004;9:629–33.
[23] Zwicker H. Evaluation of plasma parameters in optically thick plasmas. In: Lochte-Holtgreven W, editor. Plasma diagnostics. Amsterdam: North-Holland Publishing Company; 1968. p. 214–48.
[24] Griem HR. Plasma spectroscopy. New York: McGraw-Hill; 1964.
[25] Ritcher J. Radiation of hot gases. In: Lotche-Holtgreven W, editor. Plasma diagnostics. Amsterdam: John Wiley & Sons Inc.; 1968. p. 9–20.
[26] Griem HR. Spectral line broadening by plasmas. New York, USA: Academic Press; 1974.
[27] Aguilera JA, Aragón C. Characterization of a laser-induced plasma by spatially resolved spectroscopy of neutral atom and ion emissions. Comparison of local and spatially integrated measurements. Spectrochim Acta Part B 2004;59:1861–76.
[28] NIST Electronic Database. ⟨http://physics.nist.gov/PhysRefData⟩.
[29] Cremers DA, Radziemsky LJ. Laser plasmas for chemical analysis. In: Radziemsky LJ, Solarz RW, Paisner JA, editors. Laser spectroscopy and its applications. New York: Marcel Dekker; 1987.
[30] Bredice F, Borges FO, Sobral H, Villagran-Muniz M, Di Rocco HO, Cristoforetti G, et al. Evaluation of self-absorption of manganese emission lines in laser induced breakdown spectroscopy measurements. Spectrochim Acta Part B At Spectrosc 2006;61(12):1294–303.
[31] Aguilera JA, Bengoechea J, Aragón C. Curves of growth of spectral lines emitted by a laser-induced plasma: influence of the temporal evolution and spatial inhomogeneity of the plasma. Spectrochim Acta Part B 2003;58:221–37.